J Nanopart Res (2020) 22: 156
https://doi.org/10.1007/s11051-020-04878-8

RESEARCH PAPER

Thin-layer g-C_3N_4 nanosheet decoration with MoS_2 nanoparticles as a highly efficient photocatalyst in the H_2 production reaction

Mohammad W. Kadi · Reda M. Mohamed · Adel A. Ismail

Received: 19 January 2020 / Accepted: 8 May 2020 / Published online: 8 June 2020

Abstract g-C_3N_4 (graphitic carbon nitride) is an interesting photocatalyst that has found application in many fields especially in photocatalysis. It can be synthesized by various methods, and cocatalysts can be incorporated in its structure to construct a composite suitable for the desired application. We report synthesis of thin-layer g-C_3N_4 nanosheet decoration with MoS_2 nanoparticles for the preparation of 2D-2D MoS_2/g-C_3N_4 nanocomposite that was successfully used in evolution of H_2 from the reaction of water splitting. Various percentages of MoS_2 decorations were produced, and the 1.5% MoS_2 composition proved to be the best photocatalyst producing 10,000 μmol h^{-1} g^{-1} rates of H_2 evolution. The high photocatalytic activity of 2D-2D MoS_2/g-C_3N_4 is attributed to many factors that include high surface area, the 2D-2D interfaces characterized by "surface contact" active sites for absorption of light, the powerful charge separation resulting from the favorable potential values of graphitic carbon nitride nanosheets, and the use of the efficient hole-scavenger glycerol. This study shows that changes in synthesis route and careful selection of glycerol as a scavenging material can result in superior photocatalytic efficiency of the material.

Keywords 2D-2D MoS_2/g-C_3N_4 · Nanostructured photocatalyst · H_2 evolution · Visible light · Nanostructured catalysts

This article is part of the topical collection: Nanotechnology in Arab Countries, Guest Editor: Sherif El-Eskandarany

M. W. Kadi · R. M. Mohamed
Department of Chemistry, Faculty of Science, King Abdulaziz University, P. O. Box 80203, Jeddah 21589, Kingdom of Saudi Arabia

R. M. Mohamed (✉) · A. A. Ismail
Advanced Materials Department, Central Metallurgical R&D Institute, CMRDI, P. O. Box 87, Helwan, Cairo 11421, Egypt
e-mail: redama123@yahoo.com

A. A. Ismail (✉)
Nanotechnologyand Advanced Materials Program, Energy & Building Research Center, Kuwait Institute for Scientific Research (KISR), P. O. Box 24885, 13109 Safat, Kuwait
e-mail: adelali141@yahoo.com

Introduction

Hydrogen is a very attractive energy source as its use results in only water vapor emission with no other emissions. On the other hand, current practices for H_2 production require an energy source which is usually fossil fuels that generate harmful carbon and other emissions. A promising H_2 generation route is the artificial photosynthesis which research shows that it is a promising way to produce H_2 by exploiting the sun and a photocatalyst (Xiao et al. 2019; Ismail and Bahnemann 2014). If this can be realized at an industrial scale, then we will have clean energy at both ends. Finding or fabricating an efficient photocatalyst is by far the one obstacle preventing achievement of this endeavor. Research in this area is of interest to the scientific community, and many researchers publish numerous methods and materials of enhanced photocatalytic activity. A perfect photocatalyst would be of low cost, with a bandgap that favors absorption of

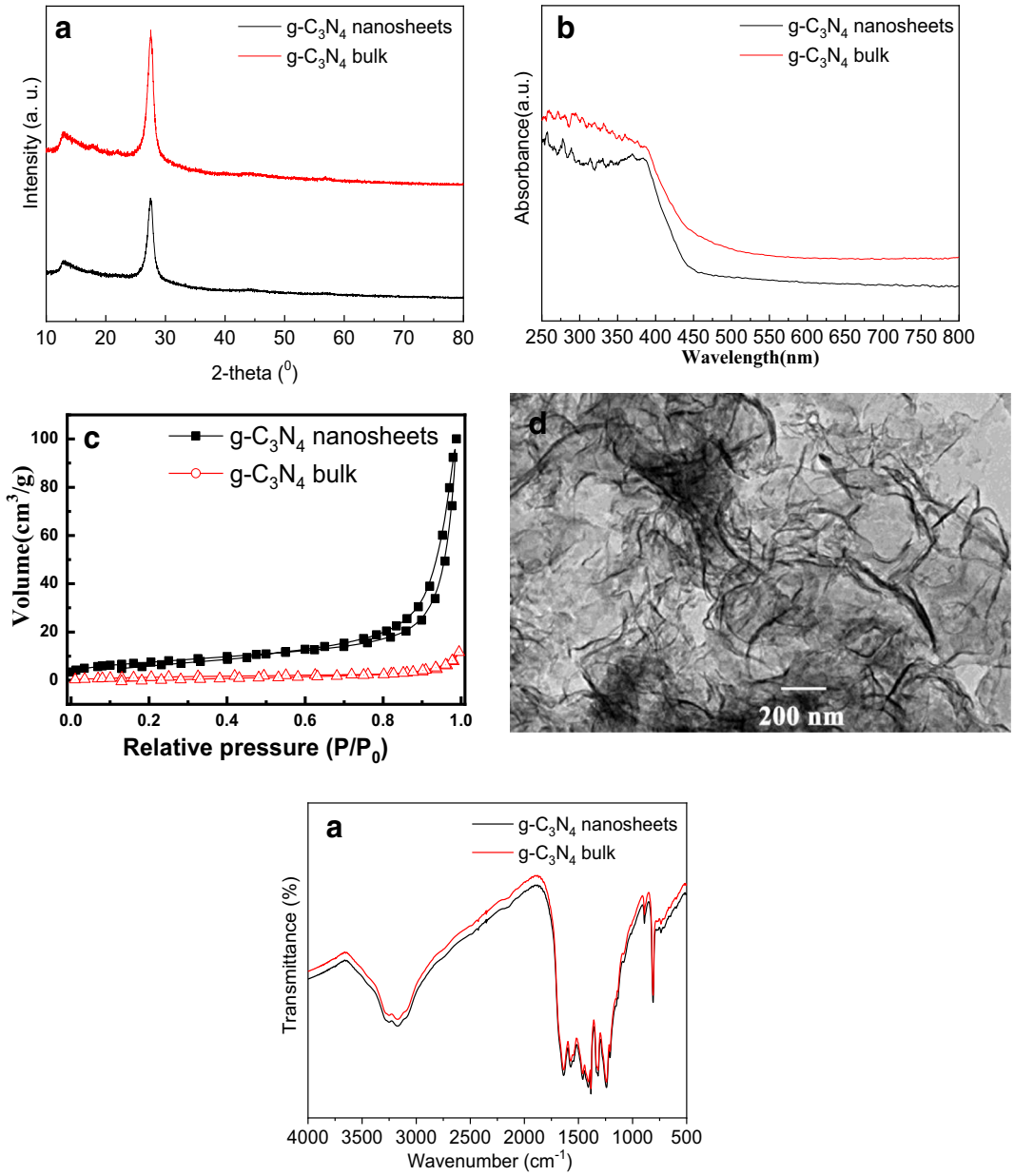

Fig. 1 XRD patterns (**a**), UV-Vis spectra (**b**), adsorption-desorption isotherm (**c**), TEM image (**d**), and FT-IR spectra (**e**) of bulk g-C_3N_4 and g-C_3N_4 nanosheets

visible light, durable, and very efficient in radiation harvesting for a sustainable photocatalytic reaction.

An interesting material that caught researchers' attention is the graphitic carbon nitride with a general formula of g-C_3N_4 as it is a visible-light absorber due its suitable band edge position (Xia et al. 2018). However, g-C_3N_4 fabricated by conventional chemical routs such as polycondensation of carbon and nitrogen-containing suffers from unfavorable properties that hinder its effective operation as efficient visible-light photocatalyst. The reason being large particle sizes reduced surface area resulting from agglomeration at high temperatures. Careful control of morphology of g-C_3N_4 during synthesis can result in a high surface area well-defined 2D sheet-structure in the nanoscale and a short diffusion length which results in great active sites number available for the reaction compared with the conventionally prepared material (Yuan et al. 2018a, b). A

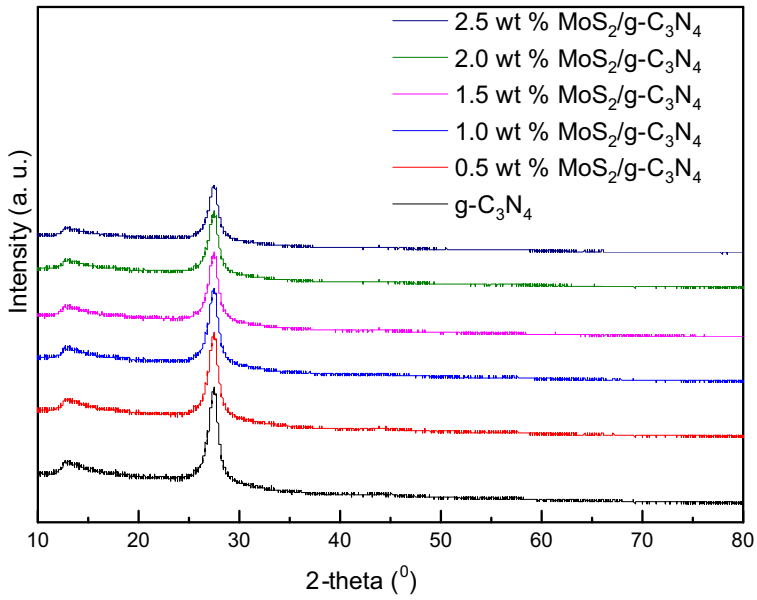

Fig. 2 XRD patterns of g-C_3N_4 and MoS_2/g-C_3N_4 nanosheets

reduced recombination probability of the charge carriers is also achieved which is translated into higher efficiency of the photocatalyst. Latterly, many approaches have been developed to fabricate 2D g-C_3N_4 structures (Zhang et al. 2018). A single atomic layered g-C_3N_4 nanosheet was successfully synthesized by an exfoliation method using conc. H_2SO_4 as a solvent (Cheng et al. 2015). However, structural integrity of the g-C_3N_4 sheet was compromised as hydrogen bonds between the units shattered by the action of the strong acid rendering the g-C_3N_4 nonplanar. The transformation of bulk graphitic carbon nitride into graphitic carbon nitride nanosheets was carried out using a simple thermal exfoliation method (Niu et al. 2012). It is obvious that harsh synthesis conditions will compromise the important properties of g-C_3N_4 sheets lowering its efficiency in the desired applications. A successful transformation of bulk graphitic carbon nitride into graphitic carbon nitride was carried out using a simple liquid exfoliation method that yielded uniquely structured g-C_3N_4 nanosheets with minimal thickness and favorable bandgap. The huge surface area available in graphitic

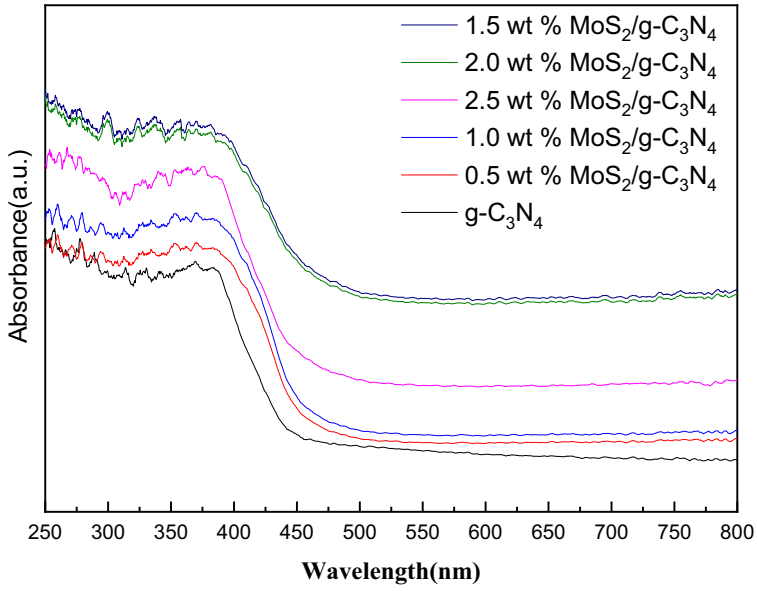

Fig. 3 UV-Vis spectra of g-C_3N_4 and MoS_2/g-C_3N_4 nanosheets

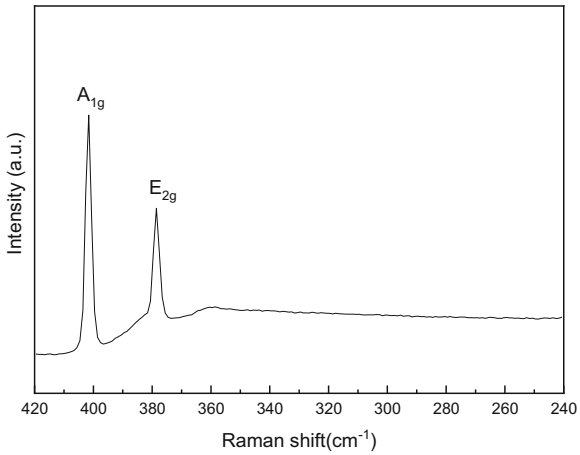

Fig. 4 Raman spectra of 1.5% MoS_2/g-C_3N_4 nanosheets

carbon nitride nanosheets can be exploited to build 2D-2D photocatalysts with the introduction of a cophotocatalyst. These structures can accommodate increased number of charge transfers which orderly enhance the photocatalytic activity of the nanocomposite (Yang et al. 2013a, b). Inspired by these new routes, in this point, we report fabrication and design and of 2D-2D MoS_2/g-C_3N_4 nanosheet photocatalyst superior in photocatalytic ability when enforced to the H_2 evolution reaction. The 2D g-C_3N_4 nanosheets are prepared by urea pyrolysis resulting in bulk g-C_3N_4 which then is transformed into thin-layer nanosheets by liquid exfoliation using polyvinylpyrrolidone and sonication. The 2D graphitic carbon nitride nanosheets were used as substrate on which MoS_2 cocatalyst nanoparticles were decorated. The thin-layer MoS_2 makes an excellent cocatalyst due to its high reactivity, suitable bandgap position, noble-metal-free composition, and low cost (Kadi et al. 2020; Yuan et al. 2019). Upon application in the water-splitting reaction, the 2D-2D MoS_2/g-C_3N_4 nanosheets yielded evolution rate of hydrogen of 10,000 μmol h^{-1} g^{-1}, superior to results obtained from MoS_2 loaded bulk graphitic carbon nitride. The synthesis method was used to produce an efficient low-cost and ecofriendly semiconductor-based photocatalyst that can be used for visible-light H_2 evolution using 2D nano junction as an efficient charge transfer medium.

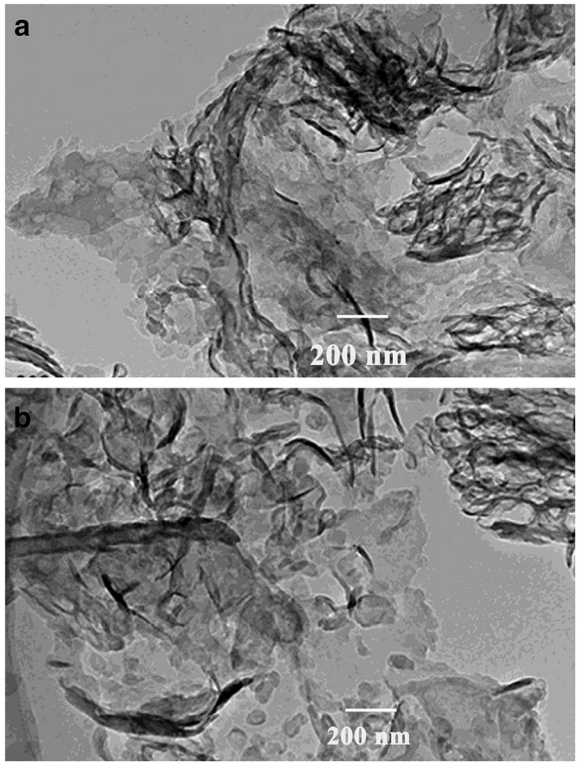

Fig. 5 TEM images of 1.0% MoS_2/g-C_3N_4 nanosheet (**a**) and 1.5% MoS_2/g-C_3N_4 nanosheet (**b**) samples

Experimental section

To achieve a highly regulated nanosheet structure, a three-phase synthesis process was followed for preparation of MoS_2/g-C_3N_4 photocatalyst. First, g-C_3N_4 nanosheets were prepared. Second, MoS_2 nanoparticles were prepared. Finally, deposition of the nanoparticles onto nanosheets was conducted.

g-C_3N_4 nanosheet synthesis

Reagents used were of analytical grade and were used as received without further purification. Bulk graphitic carbon nitride was synthesized by direct pyrolysis of 12 g of urea in a covered crucible for 3 h at 550 °C. The resultant bulk g-C_3N_4 was dispersed into polyvinylpyrrolidone (PVP) solution which was then irradiated with 4-s pulses of ultrasonic waves. Separation time between pulses was 2 s and the process was conducted for 10 h at below 4 °C using a 150-W BJED-20150 ultrasonic cell disruptor (Beijing Ultrasonic). The use of PVP in this manner proved to be fruitful in producing highly regulated few-layer nanosheets g-C_3N_4. A two-

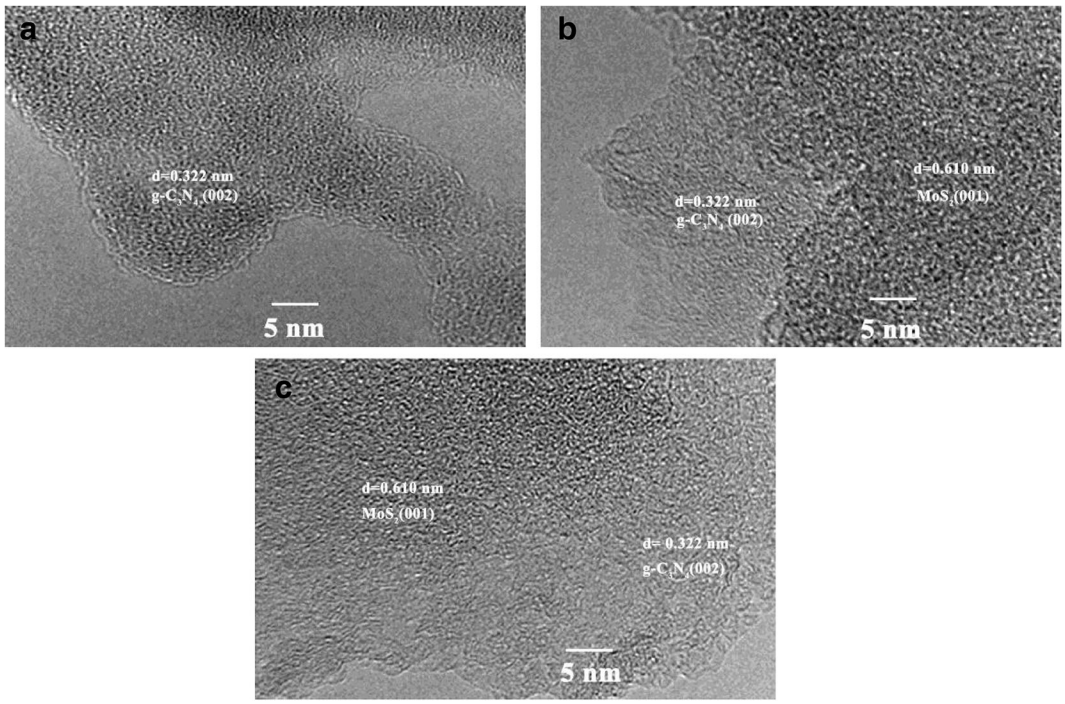

Fig. 6 HRTEM images of g-C_3N_4 nanosheet (**a**) and 1.0% MoS_2/g-C_3N_4 nanosheet (**b**) and 1.5% MoS_2/g-C_3N_4 nanosheet (**c**) samples

stage 5000- and 12,000-rpm centrifugation was employed to separate the nanosheets from the remainder of the bulk g-C_3N_4 in the mix.

MoS_2 nanoparticle synthesis

In a typical hydrothermal fashion, 4.3 g thiourea and 2 g of ammonium molybdate were dissolved in deionized water (60 mL) in Teflon-lined autoclave (100 mL) which they were set for 20 h at 200 °C. After synthesis, impurities were removed centrifugally and the pure product was dried at 100 °C for 24 h.

Preparation of MoS_2/g-C_3N_4 nanocomposites

Two grams of the thin-layer graphitic carbon nitride nanosheets was scattered into deionized water (50 mL) in a beaker. One milliliter of 3 mg/mL MoS_2 solution was next dropwise combined to the beaker using magnetic stirring which was continued for 1 h followed by 2-h ultrasonication. Solvents were then evaporated at 100 °C for 24 h. The final MoS_2/g-C_3N_4 composite powder material was produced by grinding then heating under N_2 atmosphere for 4 h at 300 °C.

Photocatalytic performance for hydrogen evolution reaction

In this process, O_2 in the water was purged using argon gas. A reaction mixture of 50 mg 1.5 wt% MoS_2/g-C_3N_4 was dispersed in glycerol solution (200 mL and 10 vol%) and was added to the 250-mL Pyrex photoreactor. Visible-light irradiation was achieved by Xenon arc lamp 500 W employing a UV-cutoff filter to ensure illumination by visible light only. Hydrogen yield was monitored hourly using Agilent 890A gas chromatograph.

Instrumentation and characterization

Bruker axis D8; JEOL-JEM-1230; Thermo Scientific K-ALPHA spectrometer; Nova 2000 series Chromatech; Shimadzu RF-5301 fluorescence spectrophotometer; V-570 spectrophotometer, Jasco, Japan; Zahner Zennium electrochemical workstation; and JASCO RFT-6000 spectrometer were employed to observe XRD patterns, shapes and sample dimensions, XPS spectra, surface area, emission photoluminescence spectra, UV-Vis-DRS spectra and bandgap information, transient photocurrent measurements, and Raman spectra respectively. All instruments were set up as

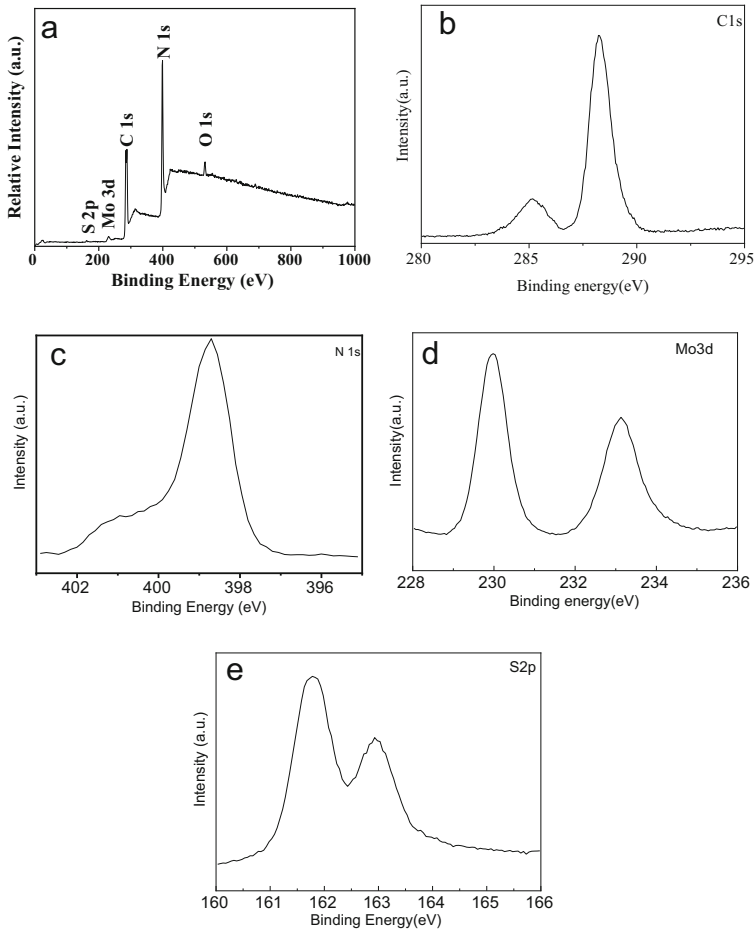

Fig. 7 XPS spectra of 1.5% MoS_2/g-C_3N_4 nanosheets, where XPS survey spectra (**a**), high-resolution XPS spectra of C1s (**b**), high-resolution XPS spectra of N1s (**c**), high-resolution XPS spectra of Mo3d (**d**), and high-resolution XPS spectra of S2p (**e**)

recommended by manufacturers to achieve best possible observations.

Results and discussions

Thin-layer g-C_3N_4 nanosheet characteristics

It is well settled that bulk g-C_3N_4 is characterized by a peak at 13.3° assigned (100) and 27.4° assigned (002) respectively (JCPDS No. 87–1526) (Cao et al. 2014). The 002 peak identifies the conjugated aromatic systems interlayer stacking in the bulk g-C_3N_4 (Yang et al. 2013a, b). When a thin layer of 2D g-C_3N_4 nanosheets is exfoliated from the bulk g-C_3N_4, the 002 peak diminishes in intensity as shown in Fig. 1 indicating that the stack thickness has shrunk. Bandgap values deduced from $(\alpha hv)^{1/2}$ vs. hv plots were estimated at 2.44 eV for 2D g-C_3N_4 nanosheets and 2.67 eV for the bulk g-C_3N_4. This significant red-shift is also apparent in spectra of UV-Vis for both phases (Fig. 1b). The favorably energetically diminished bandgap of the 2D g-C_3N_4 nanosheets can be a result of quantum effects arising from the very limited number of layers constituting the material particle (Mao et al. 2013). A huge increase in surface area results in going from bulk to thin-layer structure of g-C_3N_4. Nitrogen absorption-desorption experiments and the resulting isotherms indicate a specific surface area for the 2D graphitic carbon nitride nanosheets at 120 m^2 g^{-1} compared with only 15 m^2 g^{-1} for the bulk graphitic carbon nitride (Fig. 1c). High-resolution TEM image analysis describes the morphology of 2D g-C_3N_4 nanosheets as having widths and lengths in the range 300–700 nm with the thickness of the layers estimated at approximately 9 nm (Fig. 1d). Although the successful synthesis route produces thin-layer g-C_3N_4

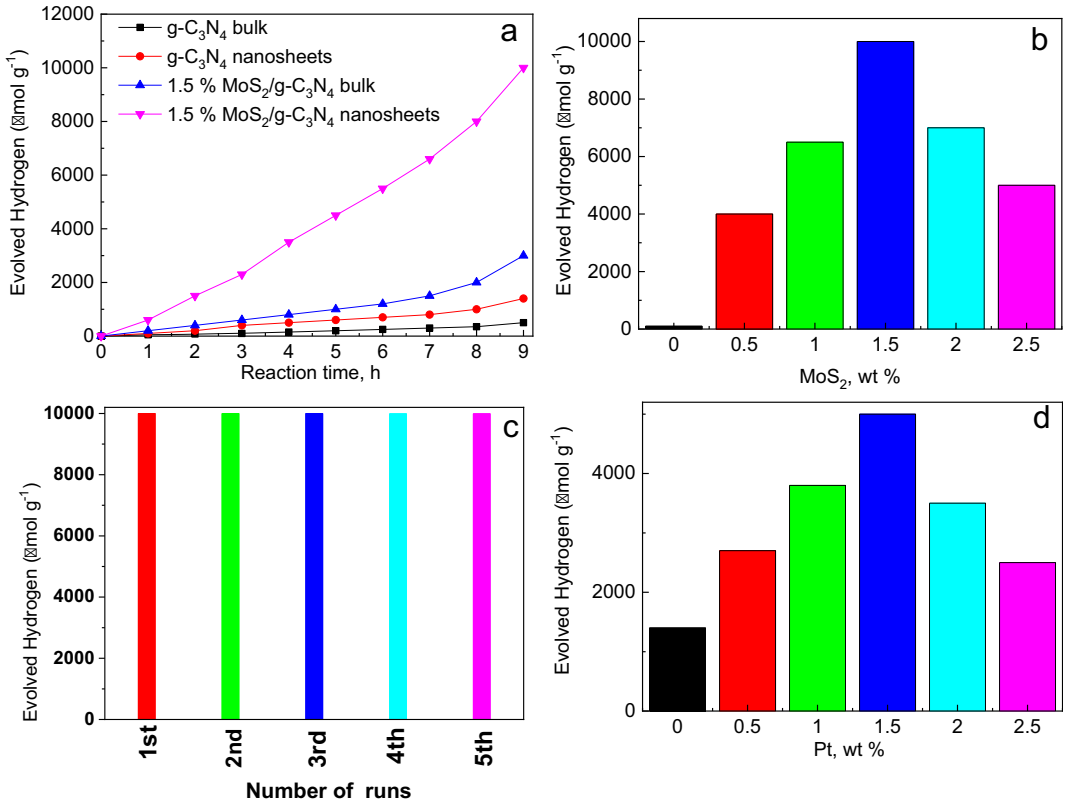

Fig. 8 **a** The H_2 evolution over different g-C_3N_4-based photocatalysts after 9 h of irradiation. **b** The effect of MoS_2 amount on the photocatalytic H_2 evolution performance. **c** Recycle H_2 generation property of 1.5% MoS_2/g-C_3N_4 nanosheet photocatalyst; after 9 h of irradiation and evacuation, the solution was irradiated again. **d** H_2 production rate of different Pt/g-C_3N_4 nanosheet photocatalysts

nanosheets, the process does not affect the crucial surface groups of the graphitic nitride as illustrated in FT-IR; these observations point to successful production of thin-layer g-C_3N_4 nanosheets. The stretching mode of triazine units was centered at 808 cm^{-1} for both samples. Also, the stretching mode of CN heterocyclic was located at ~1243, 1322, 1408, 1581, and 1633 cm^{-1} for both samples (Faisal et al. 2018). This successful transformation does not affect the important surface groups of the g-C_3N_4 as is evident from FT-IR spectra for both bulk and thin-layer g-C_3N_4 (Fig. 1e).

Thin-layer MoS_2/g-C_3N_4 nanocomposite characteristics

XRD patterns of the synthesized MoS_2/g-C_3N_4 nanocomposite do not show peaks for MoS_2, and this is probably because added MoS_2 represents a very small concentration percentage (the highest being 2.5%) that cannot be observed in the XRD spectrum (Fig. 2). It has been shown that when the concentration of MoS_2 component exceeds 10 wt%, its peaks start to show in the XRD pattern. Figure 3 shows absorption spectra of both decorated and undecorated 2D graphitic carbon nitride nanosheets. The undecorated graphitic carbon nitride nanosheets exhibit absorption at λ ~508 nm. The decorated composite shows significantly high absorption of visible light that can be referred to as MoS_2 in the structure. Two bands appear in the MoS_2/g-C_3N_4 Raman spectra (Fig. 4) at 401.4 and 378.5 cm^{-1}. These bands are characteristic of the out-of-plane A_{1g} and in-plane E_{2g} modes of 2H-MoS_2 jointly confirming decoration with MoS_2 and the presence of 2 layers per hexagonal unit cell (Fan et al. 2015). This is more proved by TEM images as they clearly show layers of MoS_2 on the surface of g-C_3N_4 nanosheets (Fig. 5). HRTEM images of pure graphitic carbon nitride, 1.0% MoS_2/g-C_3N_4, and 1.5% MoS_2/g-C_3N_4 (Fig. 6) show lattice fringes of MoS_2 with d-spacing of ca. 0.61 nm, designated to

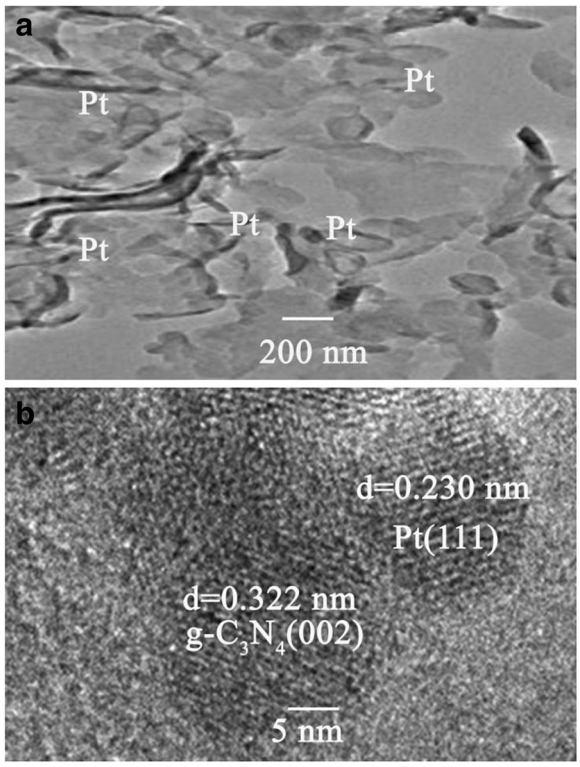

Fig. 9 **a** TEM image of 1.5% Pt/g-C_3N_4 nanosheet photocatalysts. **b** HRTEM image of 1.5% Pt/g-C_3N_4 nanosheet photocatalysts

the (001) lattice plane of hexagonal MoS_2 crystal (Yuan et al. 2018a, b) and g-C_3N_4 lattice fringes of d-spacing of ca. 0.322 nm designated to the (002) lattice plane of the g-C_3N_4.

Detailed examination of XPS spectra of the 1.5% MoS_2/g-C_3N_4 nanosheets (Fig. 7a) reveals C, N, Mo, and S elemental peaks 288.1, 398.9, 229.2, and 162.1 eV binding energies respectively (Zou et al. 2018). The 288.2 and 285.1 eV peaks (Fig. 7b) are attributed to sp^2 and sp^3 hybridization of the C atom in the structure. Deconvolution of the N1s spectrum (Fig. 7c) results in 401.2 and 399.1 eV peaks assigned to the N-(C_3) and C–N=C groups. Deconvolution of Mo 3d spectrum (Fig. 7d) results in a 3d3/2 peak at 233.0 eV and Mo 3d5/2 peak at 229.9 eV (He et al. 2018). In S 2p spectra of MoS_2, the peak at 162.9 eV is assigned to S 2p1/2, while the peak at 161.7 is assigned to S 2p3/2 (Fig. 7e) (Wang et al. 2017). All these assignments indicate successful MoS_2 decoration on g-C_3N_4 surface. The overall characterization of the synthesized MoS_2/g-C_3N_4 nanosheets reveals a structure of 2D-2D with very high surface area that points to an excellent candidate for an efficient photocatalyst.

Encouraged by the favorable characteristics of the synthesized MoS_2/g-C_3N_4 nanosheets towards photocatalysts, water-splitting photocatalytic reaction under visible-light illumination was conducted using bulk graphitic carbon nitride and the MoS_2-decorated graphitic carbon nitride nanosheets as photocatalysts and glycerol as a scavenger. Bulk graphitic carbon nitride and graphitic carbon nitride nanosheets produce rates of hydrogen evolution of 500 and 1000 μmol $h^{-1}g^{-1}$, respectively. While after decoration, the 1.5% MoS_2/g-C_3N_4 a remarkable 10,000 μmol $h^{-1}g^{-1}$ rate of evolution can be observed. Even though the bulk graphitic carbon nitride has an absorption stronger than that of graphitic carbon nitride nanosheets in the visible-light region (Fig. 8a), the larger surface area of graphitic carbon nitride nanosheets overcomes this advantage rendering graphitic carbon nitride nanosheets a more efficient photocatalyst when applied in the water-splitting reaction (Fig. 8a).

To verify the effect of MoS_2 decoration on the photocatalytic efficiency of the nanocomposite, the reaction was performed employing various percentage concentrations of MoS_2. Pure MoS_2 is an inactive photocatalyst in the H_2 production reaction while graphitic carbon nitride nanosheets exhibit weak activity with 1400 μmol h^{-1} g^{-1} rate of evolution (Fig. 8b). Upon decoration, the H_2 evolution rate increases 2.85, 4.64, and 7.14 times for 0.5%, 1.0%, and 1.5% MoS_2/g-C_3N_4 respectively compared with that of pure g-C_3N_4 nanosheets. The 1.5% MoS_2/g-C_3N_4 produced H_2 evolution rate of 10,000 μmol h^{-1} g^{-1} which is higher than all other compositions. Further increase of the MoS_2 content results in a drop in the hydrogen evolution rate. It appears that the degree of light absorption plays an essential role in determining the ultimate efficiency of the catalyst (Zou et al. 2017). When MoS_2 content increases beyond 1.5%, the number of exposed active sites on the surface of g-C_3N_4 nanosheets starts to decrease blanketed by MoS_2 causing inhibition of light absorption.

The structural stability of the photocatalyst was studied by repeating the use of 1.5% MoS_2/g-C_3N_4 nanosheets five times using 10% vol glycerol aqueous solution. H_2 evolution rate remains comparable with that of the photocatalyst when used for the first time indicating large structural stability of MoS_2/g-C_3N_4 nanosheets (Fig. 8c). The decline of glycerol concentration in the

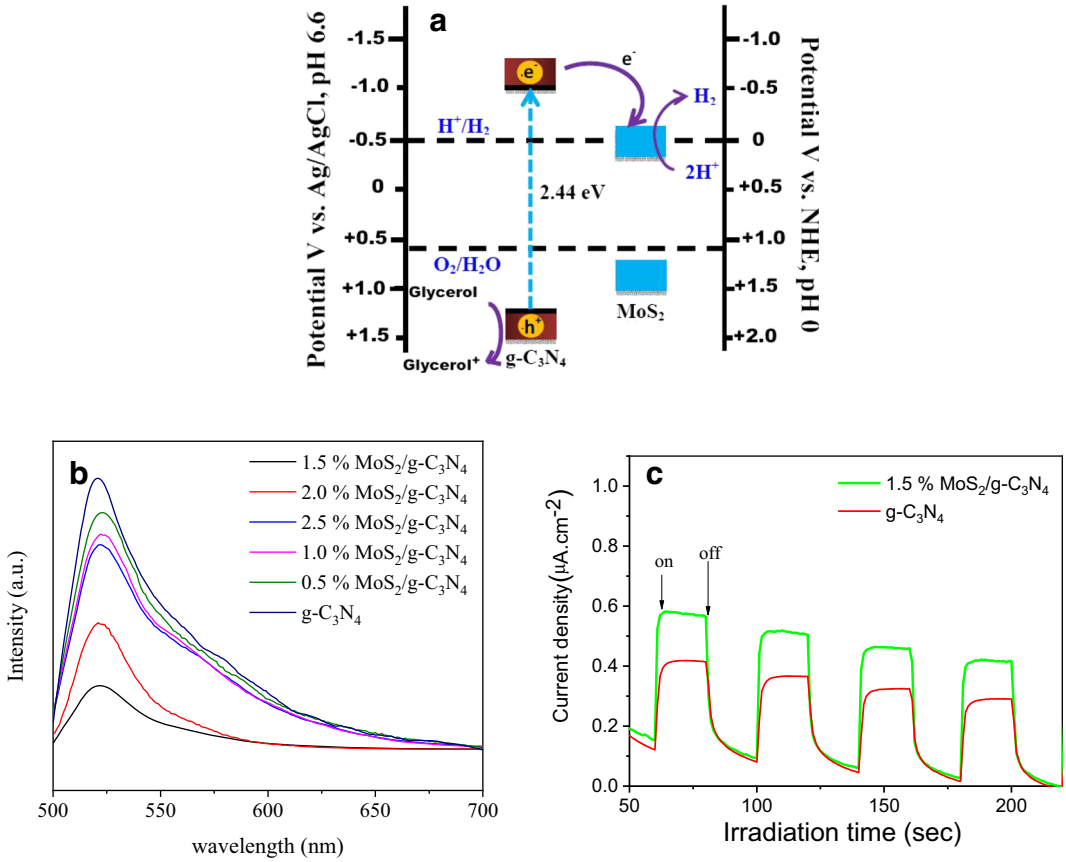

Fig. 10 **a** The reaction mechanism for photocatalytic H_2 production over $MoS_2/g\text{-}C_3N_4$ nanosheet photocatalysts. **b** Photoluminescence spectra of $g\text{-}C_3N_4$ and $MoS_2/g\text{-}C_3N_4$ nanosheets. **c** Transient photocurrent response of $g\text{-}C_3N_4$ and 1.5% $MoS_2/g\text{-}C_3N_4$ nanosheet photocatalysts

reaction mixture upon reuse could result in a slight drop in H_2 generation rate (Zhou et al. 2013). Furthermore, loss of proton from the glycerol ion or its decomposition results in gradual pH change which in turn affects the H^+/H_2 potential of reduction in addition to showing the observed decrease in the H_2 evolution rate (Lu et al. 2017).

Platinum nanoparticles are well established as highly efficient photocatalysts in the reaction of hydrogen evolution and often are used as a benchmark for activity comparison (Cao et al. 2018). We decorated the graphitic carbon nitride nanosheets with Pt nanoparticles by a photo-deposition method. Upon application of 1.5% Pt/$g\text{-}C_3N_4$ in the reaction, the maximum achieved rate of H_2 evolution was 5000 μmol h^{-1} g^{-1} which is half the value observed with the use of the optimized $MoS_2/g\text{-}C_3N_4$ nanosheet photocatalyst (Fig. 8d). The superior activity of $MoS_2/g\text{-}C_3N_4$ can be explained by examining morphology of surface of both photocatalysts. Pt/$g\text{-}C_3N_4$ nanosheets were filtered from the reactor after 9 h employment in the reaction and investigated by TEM (Fig. 9a, b). The image shows nanoparticles with 5–10 nm size range decorated on the surface of graphitic carbon nitride with a zero-dimension–two-dimension Pt/$g\text{-}C_3N_4$ structure. The Pt/$g\text{-}C_3N_4$ zero-dimension–two-dimension performs as "point contact" photocatalyst while the $MoS_2/g\text{-}C_3N_4$ two-dimension–two-dimension structure works as "face contact" photocatalyst allowing vast number of interfaces that act as powerful charge transfer medium hence the superior photocatalytic efficiency.

The reaction mechanism for photocatalytic H_2 production over $MoS_2/g\text{-}C_3N_4$ nanosheet photocatalysts is displayed in Fig. 10a. Potential values of valence bands and conduction of graphitic carbon nitride nanosheets at + 2.04 V and − 0.40 V enable it as light-harvesting medium which generates electron-hole pairs upon efficient light absorption. Once generated, the photoelectrons get

transferred to MoS_2 decoration as it has a more positive value of the potential of conduction band than that of g-C_3N_4. As we stated earlier, the 2D interfaces in the MoS_2/g-C_3N_4 structure consider as an efficient charge transfer medium allowing the much sought-after charge separation in this type of reaction. The energy resulting from photoelectron and hole recombination is emitted and can be measured using photoluminescence and time-decay fluorescence. Figure 10 b shows that peak intensity of MoS_2/g-C_3N_4 nanosheet photocatalysts downturns with the increase in MoS_2 content. The efficient transfer of photoelectrons to MoS_2 is exhibited in the diminished PL intensity. This charge separation mechanism is also confirmed from transient photocurrent response of g-C_3N_4 and 1.5% MoS_2/g-C_3N_4 (Fig. 10c). Upon addition of MoS_2, the transient photocurrent response increases indicating its charge separation ability. Upon reception of the photoelectron, MoS_2 reduces protons resulting in H_2 evolution. With its less positive oxidation potential (E ($glycerol^+$/glycerol) = + 0.2 V), glycerol gets oxidized by the positive hole regenerating the g-C_3N_4 nanosheet ground state.

Conclusion

High surface thin-layer g-C_3N_4 nanosheets were prepared and decorated by MoS_2. The synthesized nanocomposite was used as a photocatalyst in the hydrogen production reaction from water splitting using glycerol as a scavenger. The use of 1.5% MoS_2/g-C_3N_4 in the water-splitting reaction produced a rate of hydrogen evolution of 10,000 μmol h^{-1} g^{-1} which is twice the rate of the benchmark Pt/g-C_3N_4 nanosheet photocatalyst. The superior performance is coming from the high surface area of g-C_3N_4 nanosheets and the large two-dimension–two-dimension interface between g-C_3N_4 and MoS_2. This work displays that this type of two-dimension–two-dimension structure manifested in the synthesized MoS_2/g-C_3N_4 nanocomposites could be applied efficiently in photocatalysis.

Funding information This project was funded by the Deanship of Scientific Research (DSR) at King Abdulaziz University, Jeddah, under grant no. RG-26-130-38. The authors, therefore, acknowledge with thanks DSR for technical and financial support.

Compliance with ethical standards

Conflict of interest The authors declare that they have no conflict of interest.

References

Cao Y, Zhang Z, Long J, Liang J, Lin H, Lin H, Wang X (2014) Vacuum heat-treatment of carbon nitride for enhancing photocatalytic hydrogen evolution. J Mater Chem A Mater Energy Sustain 2:17797–17807

Cao Y, Wang D, Lin Y, Liu W, Cao L, Liu X, Zhang W, Mou X, Fang S, Shen X, Yao T (2018) Single Pt atom with highly vacant d-orbital for accelerating photocatalytic H2 evolution. ACS Appl Energy Mater 1:6082–6088

Cheng F, Wang H, Dong X (2015) The amphoteric properties of g-C3N4 nanosheets and fabrication of their relevant heterostructure photocatalysts by an electrostatic reassembly route. Chem Commun 51:7176–7179

Faisal M, Ismail AA, Harraz FA, Al-Sayari SA, El-Toni AM, Al-Assiri MS (2018) Fabrication of highly efficient visible light responsive TiO_2/C_3N_4 nanocomposites with enhanced photocatalytic activity. J Mol Struct 1173:428–438

Fan X, Xu P, Zhou Y, Sun YC, Li MAT, Nguyen M, Terrones TE, Mallouk (2015) Fast and efficient preparation of exfoliated 2H MoS_2 nanosheets by sonication-assisted lithium intercalation and infrared laser-induced 1T to 2H phase reversion. Nano Lett 15:5956–5960

He L, Cui B, Liu J, Wang M, Zhang Z, Zhang H (2018) Fabrication of porous CoOx/mC@MoS_2 composite loaded on g-C_3N_4 nanosheets as a highly efficient dual electrocatalyst for oxygen reduction and hydrogen evolution reactions. ACS Sustain Chem Eng 6:9257–9268

Ismail AA, Bahnemann DW (2014) Photochemical splitting of water for hydrogen production by molecular photocatalysis: a review. Sol Energy Mater Sol Cells 128:85–101

Kadi MW, Mohamed RM, Ismail AA, Bahnemann DW (2020) H_2 production using CuS/g-C_3N_4 nanocomposites under visible light. Appl Nanosci 10:223–232

Lu D, Wang H, Zhao X, Kondamareddy KK, Ding J, Li C, Fang P (2017) Highly efficient visible-light-induced photoactivity of Z-scheme g-C_3N_4/Ag/MoS_2 ternary photocatalysts for organic pollutant degradation and production of hydrogen. ACS Sustain Chem Eng 5:1436–1445

Mao J, Peng YT, Zhang HZ, Li K, Ye QL, Zan L (2013) Effect of graphitic carbon nitride microstructures on the activity and selectivity of photocatalytic CO_2 reduction under visible light. Catal Sci Technol 3:1253–1260

Niu P, Zhang L, Liu G, Cheng HM (2012) Graphene-like carbon nitride nanosheets for improved photocatalytic activities. Adv Funct Mater 22:4763–4770

Wang M, Ju P, Li J, Zhao Y, Han X, Hao Z (2017) Facile synthesis of MoS_2/g-C_3N_4/GO ternary heterojunction with enhanced photocatalytic activity for water splitting. ACS Sustain Chem Eng 5:7878–7886

Xia PF, Liu MJ, Cheng B, Yu JG, Zhang LY (2018) Template-free synthesis of hollow G-C3N4 polymer with vesicle structure for enhanced photocatalytic water splitting. J Phys Chem C 122:3786–3793

Xiao M, Wang Z, Lyu M, Luo B, Wang S, Liu G, Cheng HM, Wang L (2019) Hollow nanostructures for photocatalysis: advantages and challenges. Adv Mater 31:1801369

Yang S, Gong Y, Zhang J, Zhan L, Ma L, Fang ZY, Vajtai R (2013a) Exfoliated graphitic carbon nitride nanosheets as

efficient catalysts for hydrogen evolution under visible light. Adv Mater 25:2452–2456

Yang S, Gong Y, Zhang J, Zhan L, Ma L, Fang Z, Vajtai R, Wang X, Ajayan PM (2013b) Exfoliated graphitic carbon nitride nanosheets as efficient catalysts for hydrogen evolution under visible light. Adv Mater 25:2452–2456

Yuan YJ, Chen DQ, Huang YW, Yu ZT, Zhong JS, Chen TT, Tu WG, Guan ZJ, Cao DP (2018a) Role of two-dimensional nanointerfaces in enhancing the photocatalytic performance of 2D-2D MoS_2/CdS photocatalysts for H_2 production. Chem Eng J 350:335–343

Yuan YJ, Yang Y, Li ZJ, Chen DQ, Wu ST, Fang GL, Bai WF, Ding MY, Yang LX, Cao DP, Yu ZT, Zou ZG (2018b) Promoting charge separation in g-C_3N_4/Graphene/MoS_2 photocatalysts by two-dimensional nanojunction for enhanced photocatalytic H_2 production. ACS Appl Energy Mater 1:1400–1407

Yuan YJ, Wang P, Li ZJ, Wu YZ, Bai WF, Su YB, Guan J, Wu ST, Zhong JS, Yu ZT, Zou ZG (2019) The role of Bandgap and interface in enhancing photocatalytic H2 generation activity of 2D-2D black phosphorus/MoS_2 photocatalyst. Appl Catal B Environ 242:1–8

Zhang JH, Hou YJ, Wang SJ, Zhu XJ, Zhu CY, Wang Z, Li CJ, Jiang JJ, Wang HP, Pan M, Su CY (2018) A facile method for scalable synthesis of ultrathin g-C3N4 nanosheets for efficient hydrogen production. J Mater Chem A Mater Energy Sustain 6:18252–18257

Zhou T, Du Y, Borgna A, Hong J, Wang Y, Han J, Zhang W, Xu R (2013) Post synthesis modification of a metal-organic framework to construct a bifunctional photocatalyst for hydrogen production. Energy Environ Sci 6:3229–3234

Zou Y, Shi JW, Ma D, Fan Z, Niu C, Wang L (2017) Fabrication of g-C_3N_4/Au/C-TiO_2 hollow structures as visible-light-driven Z-scheme photocatalysts with enhanced photocatalytic H_2 evolution. ChemCatChem 9:3752–3761

Zou Y, Shi J, Ma D, Fan Z, He C, Cheng L, Sun D, Li J, Wang Z, Niu C (2018) Efficient spatial charge separation and transfer in ultrathin g-C_3N_4 nanosheets modified with Cu_2MoS_4 as a noble metal-free co-catalyst for superior visible light-driven photocatalytic water splitting. Catal Sci Technol 8:3883–3893